Statistics of fracture surfaces

Stéphane Santucci, Knut Jørgen Måløy, and Arnaud Delaplace*
Department of Physics, University of Oslo, P. O. Box 1048 Blindern, N-0316 Oslo, Norway

Joachim Mathiesen,† Alex Hansen, and Jan Øistein Haavig Bakke
Department of Physics, Norwegian University of Science and Technology, N-7491 Trondheim, Norway

Jean Schmittbuhl‡
Institut de Physique du Globe de Strasbourg, UMR CNRS 7516, 5, rue René Descartes, F-67084 Strasbourg, France

Loïc Vanel
Laboratoire de Physique, UMR CNRS 5672, Ecole Normale Supérieure de Lyon, 46 Allée d'Italie, F-69364 Lyon, France

Purusattam Ray
Institute of Mathematical Sciences, Taramani, Chennai, 600 113, India
(Received 3 March 2006; revised manuscript received 23 October 2006; published 22 January 2007)

We analyze the statistical distribution function for the height fluctuations of brittle fracture surfaces using extensive experimental data sampled on widely different materials and geometries. We compare a direct measurement of the distribution to an analysis based on the structure functions. For length scales δ larger than a characteristic scale Λ that corresponds to a material heterogeneity size, we find that the distribution of the height increments $\Delta h = h(x+\delta) - h(x)$ is Gaussian and monoaffine, i.e., the scaling of the standard deviation σ is proportional to δ^{ζ} with a unique roughness exponent. Below the scale Λ we observe a deviation from a Gaussian distribution and a monoaffine behavior. We discuss for the latter, the relevance of a multiaffine analysis and the influences of the discreteness resulting from material microstructures or experimental sampling.

DOI: 10.1103/PhysRevE.75.016104 PACS number(s): 62.20.Mk, 81.40.Np

It is difficult to believe that there may be anything in common between the morphology of fractures in, say, concrete and aluminium, except for the qualitative statement that they both are "rough." The roughness seems very different when comparing the two materials. Studies [1–5] have shown that the scaling properties of this roughness are the same to within the measuring accuracy for not only these two materials, but for most brittle or weakly ductile materials that have been tested. The scaling properties of the roughness alluded to above, is more precisely described as the fractures being self-affine. The typical deviations Δh of the surface as a function of distance δ along the fracture surface scale as $\Delta h \propto \delta^{\zeta}$ [1–5]. It has been suggested that these scaling properties might be universal [3,4].

Most studies focus only on the scaling properties of the fracture surfaces. They give no hint of the actual statistical distribution giving rise to such a scaling. In this study, following the lines of Refs. [6,7] we go beyond a calculation of the roughness exponents and propose a statistical distribution for the height fluctuations Δh of fracture surfaces. For the various materials and geometries we analyzed, we find that the Gaussian distribution provides a complete statistical description of the morphology of fractures above a characteristic scale Λ. At small scales, we observe a fanning of the structure function scaling that shows the features of a multiaffine behavior [6,8]. We, however, reexplore this analysis and discuss its relevance in particular with respect to discreteness or discontinuities (that may arise from material microstructures or measurement limitations).

Our work is based on the analysis of experimental data obtained from various experiments on different materials. The materials have been broken in different modes and geometries and the surfaces have been analyzed along one or more directions.

First we sampled a (2+1)D fracture surface in a 3D medium. The roughness measurement of the fracture surface is obtained from the failure of a granite block from Lanhlin (France) in mode I (4 bending point failure) after an initiation notch has been machined on one side of the block [9]. The scanned area of 10 cm $\times$ 10 cm covers the complete section of the block with a grid mesh of $(\delta_0)^2 = 48\ \mu$m $\times 48\ \mu$m. Accordingly the grid size is: 2062×2063, i.e., more than 4 million data points. The profiler is optical with a laser beam of 30 μm in diameter [10]. To reduce possible optical artifacts due to mineral heterogeneity, the scanned surface comes from a high-resolution silicon mold (RTV 1570) of the granite fracture. The replica technique in a perfectly homogeneous material removes fluctuations of local optical properties and significantly improves the quality of the roughness measurement [9].

Second, we analyzed the morphology of (1+1)D fracture fronts propagating in a 3D transparent medium. Dimension

*Permanent address: LMT, Ecole Normale Supérieure de Cachan, 61 ave. de Président Wilson, F-94235 Cachan, France.
†Permanent address: Department of Physics, University of Oslo, P. O. Box 1048 Blindern, N-0316 Oslo, Norway.
‡Electronic address: Jean.Schmittbuhl@eost.u-strasbg.fr

of the fracture fronts is reduced because we consider interfacial fractures where fronts propagate (in mode I) into the annealing plane between two sandblasted plexiglas (PMMA) plates [11–14]. We have analyzed six long front lines (obtained by assembling high resolution optical images of the fronts for a crack at rest [11]) containing 17 000 pixels each, with a pixel size $\delta_0=2.6$ μm.

Finally, we studied (1+1)D fracture fronts in a quasi-2D medium. Indeed, we considered the fracture of fax paper sheets loaded in mode I at a constant force [6,15,16]. High resolution optical scans were performed on post-mortem samples. We analyzed five fronts with around 10 000 pixels each, the pixel size is $\delta_0=16$ μm.

We aim at characterizing the statistical distribution function of the height fluctuations of a fracture surface $P[h(x+\delta)-h(x)]$ and comparing it with a Gaussian distribution. However, a direct measurement of the distribution function is not always accessible due to limited statistics. Only the data set on granite experiments is large enough to perform such a direct estimate. For the others, we propose a method [17] introduced in connection with the study of directed polymers [18] that is based on the structure functions defined as the kth root of the kth moment of the increment $|\Delta h|=|h(x+\delta)-h(x)|$ on a scale δ:

$$C_k(\delta)=\langle|h(x+\delta)-h(x)|^k\rangle^{1/k}. \tag{1}$$

The average is taken over the spatial coordinate x. Now, forming the ratio between the kth structure function and the second structure function, we define the function

$$R_k(\delta)=\frac{\langle|h(x+\delta)-h(x)|^k\rangle^{1/k}}{\langle[h(x+\delta)-h(x)]^2\rangle^{1/2}}. \tag{2}$$

In the case of fluctuations Δh that are Gaussian (with a zero mean and a variance σ^2):

$$P(\Delta h)=\frac{1}{\sqrt{2\pi\sigma^2}}e^{-(\Delta h)^2/2\sigma^2}, \tag{3}$$

and with a variance of the distribution that scales as $\sigma^2 \propto \delta^{2\zeta}$ where ζ is the roughness exponent, i.e., a monoaffine scaling, Eq. (1) is easily calculated: $C_k^G(\delta)=(2\delta^{2\zeta})^{1/2}\{\Gamma[(k+1)/2]/\sqrt{\pi}\}^{1/k}$. In this case the ratios R_k^G of the structure functions become

$$R_k^G=\sqrt{2}\left(\frac{\Gamma\left(\frac{k+1}{2}\right)}{\sqrt{\pi}}\right)^{1/k}. \tag{4}$$

Note that these Gaussian ratios have prescribed values with no adjustable parameters. In particular, they are independent of σ^2, hence independent of δ and ζ. This property is constrained by the assumption of an underlying Gaussian distribution. A different underlying distribution will give rise to a different set of ratios R_k.

We computed the moment ratios normalized by the Gaussian values $R_k(\delta)/R_k^G$ for different values of k and different fracture profiles we have studied, as a function of the scale ratio δ/δ_0, where δ_0 is the pixel size (see Fig. 1). Above a characteristic length scale Λ, i.e., the crossover length scale, the ratios $R_k(\delta)/R_k^G$ converge towards a constant value equal to 1, which is the signature of a Gaussian distribution. Note that a deviation from a constant value happen for the largest values of δ/δ_0 which might be related to finite size effects. At small scales, i.e., lower than Λ, a fanning of the ratios indicates a non-Gaussian distribution.

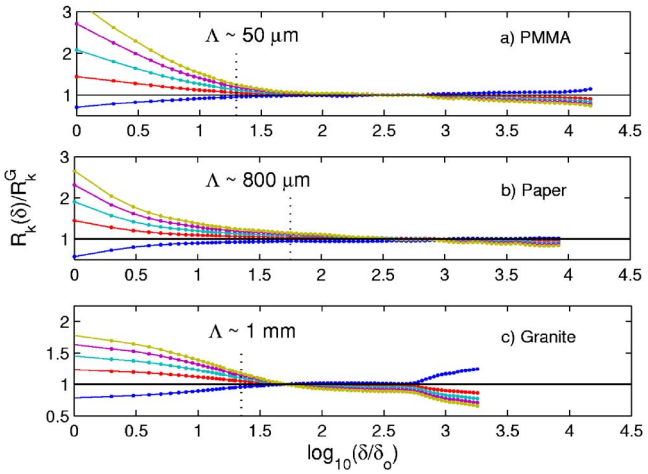

FIG. 1. (Color online) Convergence of the moment ratios R_k as a function of δ/δ_0 towards the Gaussian ratios R_k^G for the different order $k=1,2,\ldots,6$ (δ_0 is the pixel size). For each set, the individual lines visible for the small scales, represents from below to above increasing k values. The various ratios R_k are averaged over (a) six interfacial fronts in PMMA, (b) five fracture fronts in paper, and 100 profiles (c) perpendicular to the fracture propagation in a granite block. The crossover length scale is labeled Λ and estimated as the scale at which $|1-R_k/R_k^G|<5\%$, for $k=1$, 3.

It is of interest to note that the crossover length scale Λ that separates the small scale and large scale behavior of the structure functions is significantly larger than the pixel size δ_0 but similar to material microstructure length scales. Indeed, the paper fibers have a length of the order of 800 μm (their diameter being of the order of 10 μm [15]). For the PMMA experiments, the sand-blasting procedure leads to a random topography from indentation impacts at a length scale of 50 μm corresponding to the sand grain size. Minerals in granite provide also length scales. Typically their size is of the order of 1 mm. Therefore the fanning of the structure functions at small scales, most likely, reflects the microstructures of the material.

Second, we examined the scaling behavior of the structure functions. In Fig. 2 we show that the structure functions collapse above the crossover length scale Λ, when normalized by the Gaussian ratios $C_k(\delta)/R_k^G$. The collapse at the large scales provides evidence that the scaling exponent of $C_k(\delta)\sim\delta^{\zeta_k}$ is independent of k consistently with a monoaffine behavior. The roughness exponent $\zeta_k=\zeta$ previously measured for these materials [1,3–5,7,11–14] is typically obtained from tools [20] related to the second order structure functions $C_2(\delta)/R_2^G$. For a consistency check, we plot in Fig. 2 power laws with roughness exponents: $\zeta^{3D}\approx 0.8$ for the granite surface, $\zeta\approx 0.6$ for the interfacial fracture fronts in PMMA, and $\zeta^{2D}\approx 0.6$ for paper.

The fact that the rescaling by Gaussian ratios leads to a

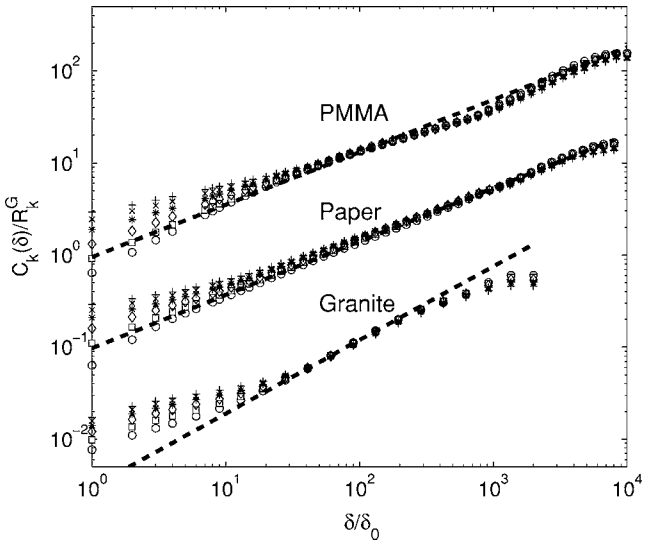

FIG. 2. Data collapse of the structure function normalized by the Gaussian ratios $C_k(\delta)/R_k^G$ for the values $k=1,2,\ldots,6$ (bottom to top curves for each material). The various data set are displaced vertically to improve the visual clarity. The dashed lines are eye guidance line based on previous extended estimated of the roughness exponent [typically based on to the second order structure functions $C_2(\delta)/R_2^G$]: for PMMA $\zeta \approx 0.6$, for paper $\zeta^{2d} \approx 0.6$ and for granite $\zeta^{3d} \approx 0.8$.

data collapse above the crossover length scales Λ, suggests that the underlying distribution is Gaussian at those scales. This result is confirmed by a direct analysis of the large data set from the fracture surface in a granite block. The analyzed data set consisted of 2000×2000 points representing the central part of a 3D map of the fracture surface to reduce boundary effects. From the map we not only computed the structure functions as shown in Fig. 2, but we also computed directly the statistical distribution of the height fluctuations $P(\Delta' h)$ at different length scales δ, where $\Delta' h = (\Delta h - \langle \Delta h \rangle)$ $\times(\delta)$. Note that we subtract the averaged height fluctuations $\langle \Delta h \rangle$ in order to center the various distributions around a zero mean. The structure functions [Eq. (1)] are defined without such a procedure. However, we checked that it did not influence the scaling behavior of the structure functions, by directly detrending the various profiles. In Fig. 3 we show the distributions of the height fluctuations for logarithmically increasing length scales δ. The data were extracted in the direction perpendicular to the fracture propagation and the distributions were sampled from the 2000 profiles $h(x)$ each containing 2000 points. We clearly see that above the characteristic length scale $\Lambda \sim 1$ mm (i.e., 20 δ_0), the shape of the distributions become Gaussian. Interestingly, a similar cross over has been observed in the width distribution of contact lines measured recently [19]. We emphasize that the self-affine behavior of the fracture front enters through the scaling of the standard deviation $\sigma \propto \delta^{\zeta^{3D}}$. We obtained from a direct estimate (see the inset in Fig. 3), $\zeta^{3D} \approx 0.75$. This estimate is typically a low side estimate of the roughness exponent [20].

At small scales (see Fig. 2), we observe a fanning of the structure functions together with a deviation from a gaussian distribution in particular for the tails of the distribution (see Fig. 3). Several authors have reported similar findings [21,22]. If one assumes that the scaling of the structure functions can be fitted by power laws, a multiscaling analysis can be performed. This has already been recently reported for the paper data [6]. Figure 4(a) shows the fits of the structure function in this framework with a linear law for the scaling exponents: $\zeta_k = H - \alpha k$ with $H = 0.64$ and $\alpha = 0.026 \pm 0.002$ [6]. (In Refs. [21,22], the definition of the structure function is different leading to a quadratic framework for the scaling exponent.) The fits are consistent for a short range of scales around the crossover length scale Λ but not at very small scales. We clearly see that corrections to scaling are significant for scales smaller than Λ.

We argue that the multi-affine-like behavior at the small-

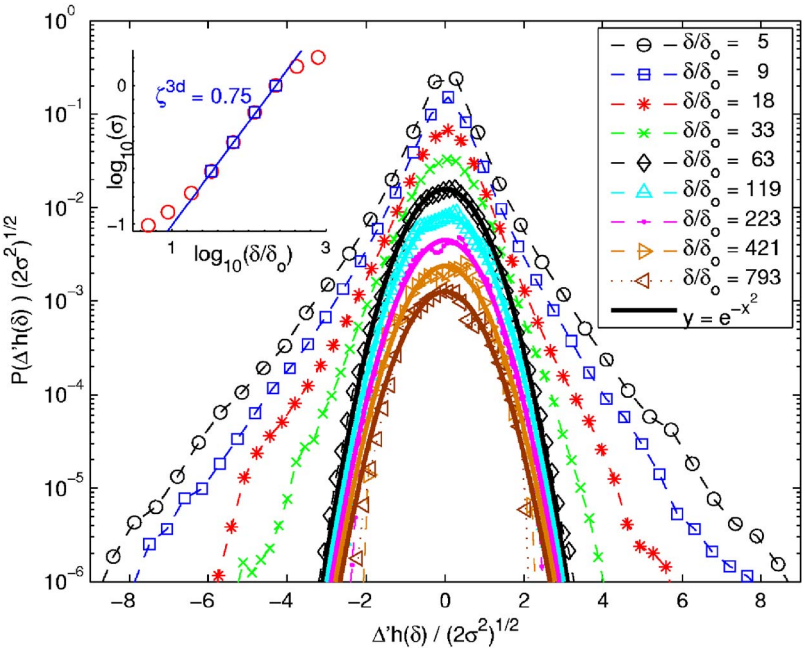

FIG. 3. (Color online) Statistical distributions of the height fluctuations $P(\Delta' h)$ sampled from a grid of 2000 lines in the direction perpendicular to the fracture propagation in a 3D granite block. We show the distribution for logarithmically increasing length scales δ. Note that in addition, we have shifted the various distributions logarithmically for visual clarity. We plot on a semilog scale $P(\Delta' h)\sqrt{2\sigma^2}$ versus $(\Delta' h)/\sqrt{2\sigma^2}$ and observe at large scales a typical parabolic shape of a Gaussian distribution. The solid lines represent the curve $y = e^{-x^2}$ and fit the experimental distributions above a characteristic length scale $\Lambda \sim 20\delta_0 \sim 1$ mm. Inset: The scaling behavior of the standard deviation of the distributions $P[\Delta' h(\delta)]$ allows us to extract the roughness of the fracture surface $\sigma \propto \delta^{\zeta^{3d}}$ with $\zeta^{3d} \approx 0.75$.

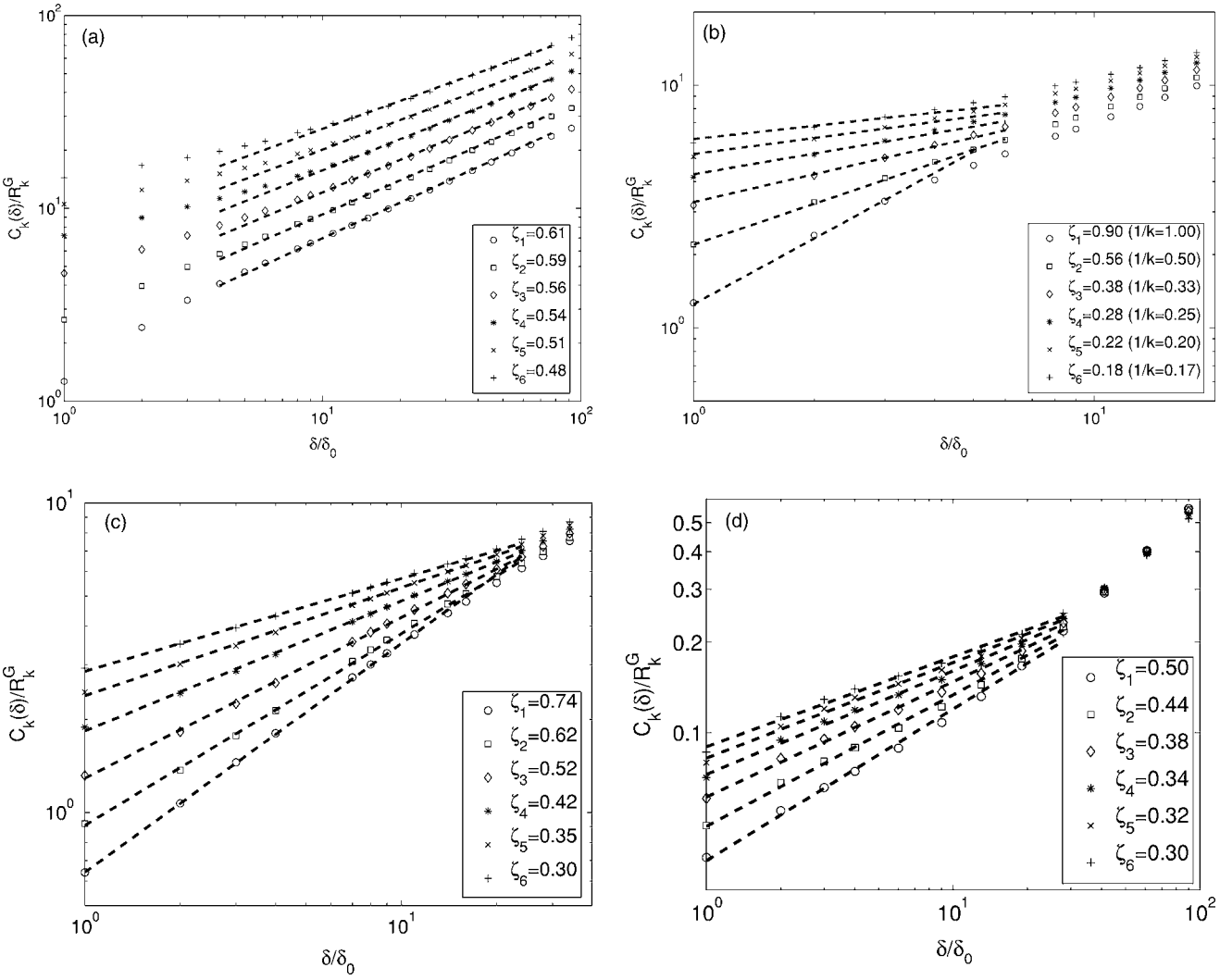

FIG. 4. Details at small scales of the structure functions C_k normalized by the Gaussian ratio R_k^G for different $k=1,2,\ldots,6$ (from bottom to top curves): (a) Paper data with power law fits based on a quadratic function of the exponent [6] (each plot has been shifted for readability); (b) same paper data but with power law fits based on a $1/k$ function of the exponent; (c) PMMA data with power law fits ($1/k$ fits are not consistent with the data.); (d) granite data with power law fits ($1/k$ fits are not consistent with the data). δ_0 is the pixel size.

est scales is possibly a result of jump discontinuities in the fracture front sampling. Such discontinuities are likely to arise from the material properties or from lack of sufficient resolution in measurement processes. Figure 5(a) shows a typical picture of a fracture in paper sheet. The line that defines the fracture front has been superimposed. Clearly the front is strongly influenced by the nonbroken fibers along the fracture. Numerous front fluctuations are related to an arbitrary definition of the front along the fiber. Accordingly, the front includes a set of vertical jumps. One important question is: what is the influence of these jumps on the scaling of the fracture front? Possibly it may have a significant contribution. Indeed, in Kardar-Parisi-Zhang (KPZ) models on kinetic surface roughening, a broadly distributed noise gives rise to rare but large perturbations of the surface and hence a multiscaling of the structure functions at small scales [21].

To illuminate the origin of such multi affine bahavior, consider a piecewise continuous fracture surface with a number of vertical jumps of size ϵ_i, e.g., due to overhangs, mi-

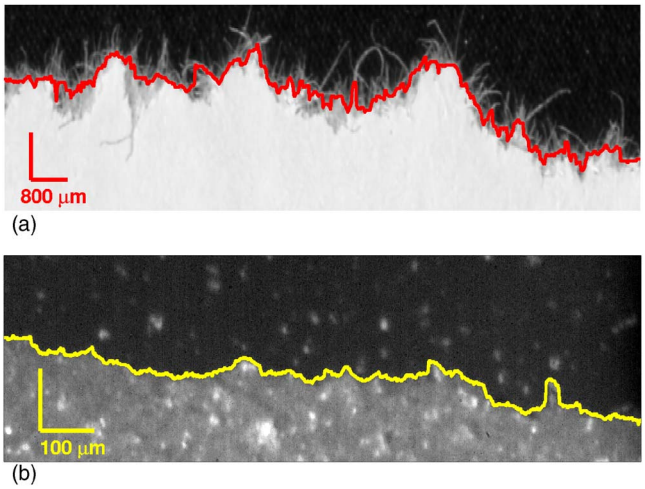

FIG. 5. (Color online) Zoom of crack front images: (a) paper sheet; (b) PMMA.

croscopical defects or the grain size in granite and the fibre size in paper. On sufficiently small length scales δ, the height variations in the surface will be negligible relative to the jump size ϵ_i. The structure function will therefore collect from each jump a contribution roughly proportional to $\delta\epsilon_i^k$ [23]. Overall, the contribution to Eq. (1) will be $C_k(\delta) \sim \delta^{1/k}(\Sigma_i \epsilon_i^k)^{1/k}$ where the sum is taken over all the jumps. We see that the structure function now scales with a k-dependent Hurst exponent $\zeta_k = 1/k$. Actually this behavior is observed for paper data, for values of k close to or larger than unity [see Fig. 4(b)] at small scales. For small values of k the effect of the vertical jumps will diminish relative to the ordinary surface roughening and therefore $\zeta_k \approx \zeta$ for $k \ll 1$.

On the contrary, the influence of the jumps is rather limited for PMMA and Granite data. Figure 5(b) shows a picture of the fracture for PMMA. No fiber emerges from the front. The crack front is more easily and precisely defined. Only limited flaws interact with the main crack front and subsequently limited jumps are present. Hence, the $1/k$ behavior is not observed for the scaling exponents of the structures functions [see Fig. 4(c)]. The granite crack surface is similar to the PMMA crack experiment in the sense that the interface is clearly defined and profiles along it contain very limited jumps. In this case, the $1/k$ behavior is also not observed [see Fig. 4(d)].

A related aspect might strongly influences the structure functions at small scales. Indeed, it is important to have in mind that the experimental scan of the surface at small scales might be spurious due to limitations of the profilometers or scanners leading, for instance, to artificial jumps in the measured profiles. The discretization (coarse graining) of the data also plays a crucial role, see Refs. [11,24]. Figure 6 demonstrates how sensitive the structure function is to the discretization. We generated graphs with roughness exponent $\zeta = 0.6$ from a fractional Brownian motion. We then filtered the graphs by representing the values of h using 3, 5, 7, and 9 bits for 2σ (see Fig. 6). When decreasing the resolution (the number of bits), we observe at small scales a clear deviation from the expected scaling behavior and more importantly a fanning of the structure functions $C_k(\delta)$. In order to check the impact of this effect on our data, we estimated in pixel unit, the magnitude of the fronts as 2σ computed over the entire fronts. We obtained for paper data, $2\sigma \approx 430$ which corresponds to almost a 9 bit measurement, for PMMA data, $2\sigma \approx 40$ which is a 5 bit measurement and for granite data, $2\sigma \approx 26\,000$ which is more than a 14 bit measurement. Subsequently, structure functions of paper and granite data are very little affected by the pixelization effect. On the contrary, for PMMA fanning is expected to come possibly from this effect.

We argue that microstructures could play a role similar to the experimental pixelization on the structure functions. Indeed, at comparable or smaller scales than the microstructure size, crack front advances are controlled by the size of the microstructures. Accessible positions of the front are limited to a set of discrete spots, especially for inter microstructure

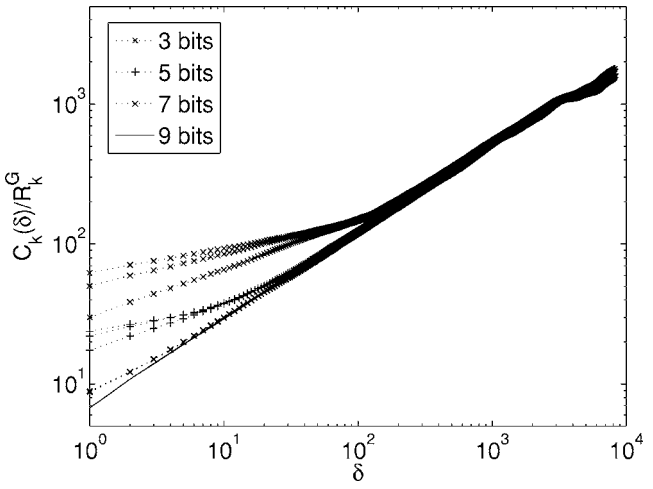

FIG. 6. Influence of the sampling resolution on the structure functions $C_k(\delta)/R_k^G$ (for k=2, 3, 4 from bottom to top curves of each resolution). A synthetic self-affine front of 16 384 points with a roughness exponent $\zeta = 0.6$, has been coarse-grained using different resolutions. Each resolution is defined by the number of bins (in bits: 3, 5, 7, or 9) required to cover two rms of h. Note that the fanning of the structure functions on the small scales diminishes as the resolution is increased.

advances. Accordingly, the fanning of the structure functions might be related to discreteness of the material.

In conclusion, we have analyzed experimental data on fracture profiles in widely different materials. The structure function ratios R_k [Eq. (4)] converge to the values of a Gaussian distribution above a characteristic scale. We have verified our findings by also computing directly the distribution of the height fluctuations and have shown that there exists a unique scaling exponent, ζ, permitting the rescaling of the height fluctuation distribution $P[\Delta h(\delta)] \sim \delta^{-\zeta} G[\Delta h(\delta)/\delta^{\zeta}]$, where the rescaling function G has a Gaussian form consistently with a monoaffine scaling. From a fundamental point of view, the distribution of the height fluctuations provides new important information about the morphology of fracture surfaces; information which is not covered by the calculations of a roughness exponent. At small scales, we observe a fanning of the structure functions that we interpret as the signature of discreteness owing to either experimental limitations or material heterogeneities and question the relevance of a multiaffine analysis.

Note added. Recently, Alava *et al.* have published a paper with similar conclusions as ours in connection with paper fracture lines [25].

We thank S.G. Roux and R. Toussaint for fruitful discussions and their critical reading of the manuscript. S. Santucci was supported by the NFR Petromax Program No. 163472/S30, J. Mathiesen was supported by Grant No. NFR-166802, J. Schmittbuhl by the EHDRA project and ANR program MODALSIS, and L. Vanel by the ANR Program No. ANR-05-JCJC-0121-01.

[1] E. Bouchaud, J. Phys.: Condens. Matter **9**, 4319 (1997).
[2] B. B. Mandelbrot, D. E. Passoja, and A. J. Paullay, Nature (London) **308**, 721 (1984); S. R. Brown and C. H. Scholz, J. Geophys. Res. **90**, 12575 (1985).
[3] E. Bouchaud, G. Lapasset, and J. Planés, Europhys. Lett. **13**, 73 (1990).
[4] K. J. Måløy, A. Hansen, E. L. Hinrichsen, and S. Roux, Phys. Rev. Lett. **68**, 213 (1992).
[5] J. Schmittbuhl, S. Gentier, and S. Roux, Geophys. Res. Lett. **20**, 639 (1990); B. L. Cox and J. S. Y. Wang, Fractals **1**, 87 (1993); F. Célarié, S. Prades, D. Bonamy, L. Ferrero, E. Bouchaud, C. Guillot, and C. Marlière, Phys. Rev. Lett. **90**, 075504 (2003).
[6] E. Bouchbinder, I. Procaccia, S. Santucci, and L. Vanel, Phys. Rev. Lett. **96**, 055509 (2006).
[7] J. Schmittbuhl, F. Schmitt, and C. Scholtz, J. Geophys. Res. **100**, 5953 (1995).
[8] L. I. Salminen, M. J. Alava, and K. J. Niskanen, Eur. Phys. J. B **32**, 369 (2003).
[9] Y. Méheust, Ph.D. thesis, Orsay University, France, 2002 (unpublished).
[10] J. Schmittbuhl, F. Renard, J. P. Gratier, and R. Toussaint, Phys. Rev. Lett. **93**, 238501 (2004).
[11] A. Delaplace, J. Schmittbuhl, and K. J. Måløy, Phys. Rev. E **60**, 1337 (1999).
[12] K. J. Måløy, S. Santucci, J. Schmittbuhl, and R. Toussaint, Phys. Rev. Lett. **96**, 045501 (2006).
[13] S. Santucci, K. J. Måløy, R. Toussaint, and J. Schmittbuhl, in *Dynamics of Complex Interconnected Biosensor Systems: Networks and Bioprocesses*, edited by A. T. Skjeltorp (Kluwer, Amsterdam, 2006).
[14] J. Schmittbuhl and K. J. Måløy, Phys. Rev. Lett. **78**, 3888 (1997); J. Schmittbuhl, A. Delaplace, K. J. Måløy, H. Perfittini, and J. P. Vilotte, PAGEOPH **160**, 961 (2003).
[15] S. Santucci, L. Vanel, and S. Ciliberto, Phys. Rev. Lett. **93**, 095505 (2004).
[16] S. Santucci, P. Cortet, S. Deschanel, L. Vanel, and S. Ciliberto, Europhys. Lett. **74**, 595 (2006).
[17] T. Halpin-Healy, Phys. Rev. A **44**, R3415 (1991).
[18] D. A. Huse and C. L. Henley, Phys. Rev. Lett. **54**, 2708 (1985); M. Kardar, *ibid.* **55**, 2235 (1985); **55**, 2923 (1985).
[19] S. Moulinet, A. Rosso, W. Krauth, and E. Rolley, Phys. Rev. E **69**, 035103(R) (2004).
[20] J. Schmittbuhl, J. P. Vilotte, and S. Roux, Phys. Rev. E **51**, 131 (1995).
[21] A.-L. Barabási, R. Bourbonnais, M. Jensen, J. Kertész, T. Vicsek, and Y.-C. Zhang, Phys. Rev. A **45**, R6951 (1992).
[22] G. M. Buendía, S. J. Mitchell, and P. A. Rikvold, Microelectron. J. **36**, 913 (2005).
[23] S. J. Mitchell, Phys. Rev. E **72**, 065103(R) (2005).
[24] J. Buceta, J. Pastor, M. A. Rubio, and F. J. de la Rubia, Phys. Rev. E **61**, 6015 (2000).
[25] Mikko J. Alava, Phani K.V.V. Nukala, and Stefano Zapperi, J. Stat. Mech.: Theory Exp. (2006) L10002.